NASA TECHNICAL NOTE

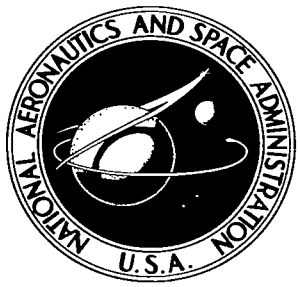

NASA TN D-3817
C. 1

NASA TN D-3817

ULTRASONIC ATTENUATION IN SUPERCONDUCTING NIOBIUM

by Joseph H. Simmons
Lewis Research Center
Cleveland, Ohio

NATIONAL AERONAUTICS AND SPACE ADMINISTRATION • WASHINGTON, D. C. • JANUARY 1967

ULTRASONIC ATTENUATION IN SUPERCONDUCTING NIOBIUM

By Joseph H. Simmons

Lewis Research Center
Cleveland, Ohio

NATIONAL AERONAUTICS AND SPACE ADMINISTRATION

For sale by the Clearinghouse for Federal Scientific and Technical Information
Springfield, Virginia 22151 – Price $1.00

ULTRASONIC ATTENUATION IN SUPERCONDUCTING NIOBIUM*

by Joseph H. Simmons

Lewis Research Center

SUMMARY

The attenuation of ultrasonic waves with frequencies between 30 and 330 megahertz was investigated in niobium single crystals oriented in the (100) and (110) crystal directions. The dependence of the attenuation on temperature was observed with the samples in different background magnetic fields, and the temperature-dependence energy gap was calculated from the observed attenuation by using the Bardeen-Cooper-Schrieffer model. The experiment was performed on both annealed and unannealed niobium single crystals. Both longitudinal and shear waves were used. The study of longitudinal waves led to a determination of the anisotropy of the zero-temperature energy gap.

INTRODUCTION

In recent years, the study of ultrasonic attenuation due to conduction electrons has provided a powerful tool for investigating the electron-lattice interaction and for determining the properties of electrons in metals. The extension of these measurements to superconductors has yielded valuable information concerning the energy gap and the electron-lattice interaction.

The Bardeen-Cooper-Schrieffer theory of superconductivity (ref. 1) developed in 1957 described the absorption of ultrasonic waves in the superconducting state and, as a consequence, initiated a large number of experiments using tin (refs. 2 to 4), aluminum (refs. 5 and 6), and lead (refs. 7 and 8) crystals. A few preliminary experiments were performed on the hard superconductors, niobium (refs. 9 to 11) and vanadium (refs. 11 and 12), but only a small range of parameters was studied. In general, a considerable range of energy-gap values was obtained in these previous investigations of hard super-

*The information presented herein was submitted as a thesis in partial fulfillment of the requirements for the degree Master of Science in Physics at John Carroll University, Cleveland, Ohio, in June 1966.

conductors. Inaccurate temperature control at low reduced temperatures, as well as amplitude dependence of the type observed in lead (ref. 7), may have contributed to the difference in results. Because of impurities and dislocations, the mean free paths ℓ of the conduction electrons were not much greater than the length $1/q$ of the imposed ultrasonic waves; consequently, only samples with mean-free-path to wavelength ratios less than or close to 1 ($q\ell \lesssim 1$) were studied.

An investigation of the attenuation of ultrasonic waves in niobium crystals was conducted with the temperature carefully controlled. A preliminary study of the amplitude-dependence effect (a change in attenuation with energy of the input signal) was undertaken in order to avoid obtaining results unrelated to the Bardeen-Cooper-Schrieffer (BCS) theory. An observation of the effect of electronic mean-free-path length was made by comparing measurements of two originally identical samples with different resistance ratios. A range of $q\ell$ values from much less than 1 to much greater than 1 was obtained by varying the frequency of the ultrasonic waves from 30 to 330 megahertz and by using annealed and commercially available niobium crystal samples.

Niobium single-crystal rods were oriented with their axes parallel to the (100) and (110) crystal directions. The dependence of attenuation on temperature was observed with samples in different background magnetic fields, and the effect of magnetic field on the type of phase transition to the normal state was investigated. The temperature-dependent energy gap was calculated from the observed attenuation by using the BCS model. Both longitudinal and shear waves were used to determine gap anisotropy. The attenuation of low-frequency, ultrasonic waves was carefully studied in an effort to observe the collective excitation modes for electrons in the superconducting state corresponding to pressure waves in a neutral Fermi gas, as seen by Claiborne and Einspruch (ref. 13).

ULTRASONIC ATTENUATION IN SUPERCONDUCTING STATE

The attenuation of ultrasonic waves in superconducting metals decreases sharply when the sample temperature is lowered below the transition temperature. This drop can be attributed to the absence of states within the energy gap, which implies that, to become excited, the superconducting electrons cannot absorb the sound energy in amounts less than the gap 2Δ. This drastically reduces the transition probability and, consequently, the attenuation. The microscopic theory developed by Bardeen, Cooper, and Schrieffer (ref. 1) explained this phenomenon for longitudinal waves. The dependence of energy gap on temperature, derived by the BCS theory, is plotted in figure 1 from values of $\Delta(T)$ obtained in reference 14. The energy gap at zero ($2\Delta(0)$) was calculated to be $3.52\, k_B T_c$. Assuming that the density of states is not changed in the transition from the normal to the

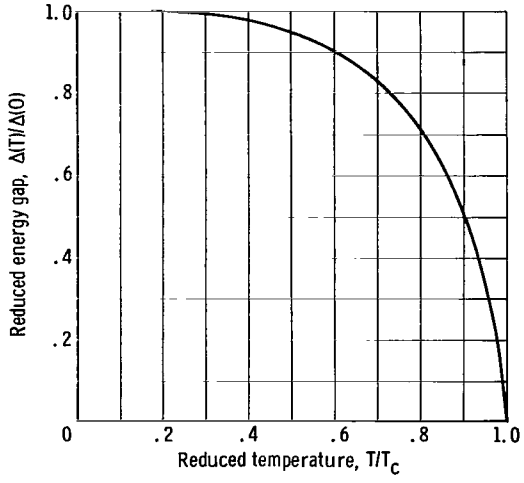

Figure 1. - Energy-gap parameter of Bardeen-Cooper-Schrieffer theory.

superconducting state, except near the gap, the BCS theory relates the ratio of the superconducting to normal attenuations with the temperature-dependent energy gap in the equation

$$\frac{\alpha_s}{\alpha_n} = \frac{f(\Delta)}{f(0)} = \frac{2}{\exp\left(\frac{\Delta(T)}{k_B T}\right) + 1} \qquad (1)$$

All symbols are defined in the appendix.

In general, good agreement exists between the attenuation equation and the experimental results. Small deviations were observed in the region of high T/T_c because the energy bands are slightly anisotropic; therefore, the attenuation actually involves a complicated average of the energy gap. However, these deviations do not impair the general usefulness of the BCS theory in the study of ultrasonic attenuation in superconductors.

Implicit in the BCS analysis through the assumption of predominance of electron-phonon interactions is the condition that $q\ell \gg 1$. Later, Tsuneto (ref. 15) derived the attenuation for arbitrary mean free paths and showed that the temperature dependence is not different from the BCS theory, including cases of $q\ell \ll 1$.

As in the case of normal metals, because of energy and momentum conservation, only electrons with group velocity components in the direction of propagation of the wave nearly equal to the sound velocity contribute in the attenuation. Since most electrons in this case have group velocities much larger than sound velocity, only those moving in directions nearly perpendicular to the sound propagation direction satisfy the condition. Therefore, the energy gap over definite regions of the Fermi surface can be measured by varying the direction of wave propagation relative to the crystal axes.

In the case of transverse ultrasonic waves, because of the Meissner effect, shielding currents are set up to counteract the phonon transverse electromagnetic fields caused by the lattice motion (ref. 14). Only small sections of the sample (of the order of the penetration depth) are affected by the ultrasonic wave; consequently, few electrons will absorb energy from it. It is then expected that the attenuation will drop abruptly just below the critical temperature. Bohm and Morse (ref. 16) observed this abrupt drop in the shear wave attenuation in polycrystalline indium and tin with $q\ell > 1$. They also observed a decrease in the magnitude of the sharp drop with descending $q\ell$ values. The reason (refs. 14 to 17) for this decrease in the sharp drop for $q\ell \ll 1$ is that local collisions become the dominant mechanism in the interaction between the electrons and the lattice. Thus, in this case, Meissner shielding has little effect in decreasing the attenuation.

GENERAL EXPERIMENTAL TECHNIQUES

Ultrasonic attenuation in a metal is studied by observing the decrease in amplitude of short-duration mechanical pulses as they are propagated back and forth through the test sample. An electrical signal first excites a transducer, which then transmits to the sample an ultrasonic pulse through a thin layer of coupling material. Successive echoes of this pulse are picked up, amplified by a receiver, and usually displayed on an oscilloscope. The energy lost by the wave while propagating over multiples of the sample length is found by using a calibrated pulse comparator to measure the attenuation difference between the echoes. The variation of energy absorption in the metal is then studied by monitoring the desired parameters.

The ultrasonic attenuation measurements described herein were made with equipment (fig. 2) of the type used by Morse (ref. 14) and Chick, Anderson, and Truell (ref. 18). A master synchronizer generates pulses which alternately trigger a pulsed oscillator and a calibrated attenuator, or pulse comparator. These pulses are also used to trigger the oscilloscope. The oscillator sends 50 to 500 pulses per second on a carrier wave which can be varied in frequency between 30 and 330 megahertz. The ultrasonic pulses are then transmitted to a quartz crystal transducer of fundamental frequency varying between 5 and 30 megahertz. The electrical pulses are transformed into mechanical pulses by the transducer and then transmitted to the sample by a coupling bond. Successive echoes of the original pulse are picked up and amplified by a receiver and then displayed on an oscilloscope screen. Two means of detecting the echoes are frequently used: the double-transducer method, which uses separate transducers to produce the pulse and pick up the

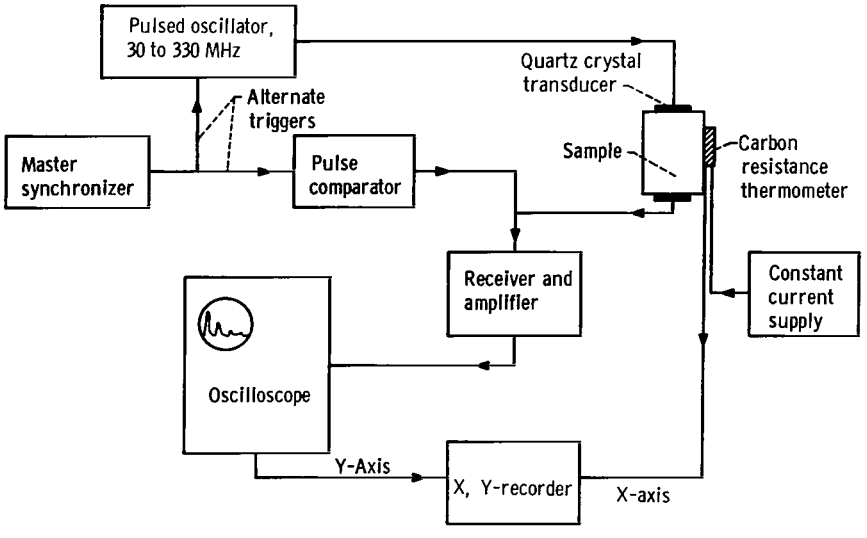

Figure 2. - Block diagram of ultrasonic equipment used in observing attenuation in niobium.

echoes, and the single-transducer method, which uses the same transducer to produce the pulse and to pick up the reflected echoes. The equipment in this experiment could be used with either method. However, because of its simplicity, the single-transducer, reflected-echo technique was used exclusively. The oscilloscope shown in figure 2 samples the visual display at any point and produces a signal proportional to the height of the sample point above a variable zero level. This signal is plotted on the Y-axis of an X, Y-recorder. A constant current source with matched transistors to eliminate the effect of thermal fluctuations was used to power the resistance thermometer, which was a 1/10-watt, 100-ohm carbon resistor. The thermometer returned to the same resistance after being cycled several times between room and liquid-nitrogen temperatures, then it was calibrated by the method of Clement and Quinnell (ref. 19). The voltage across the resistor was recorded on the X-axis of the X, Y-recorder. In this manner direct readings of the variation of attenuation with temperature were obtained. A doped germanium resistor was also used as a thermometer; however, since its sensitivity was smaller than that of the carbon resistor in the temperature range of interest, it served mainly to check the calibration of the carbon element. The temperature readings from both the carbon and germanium resistors were the same and thus indicated that no appreciable thermal gradients were present in the copper heat sink during the experiments. The variable-

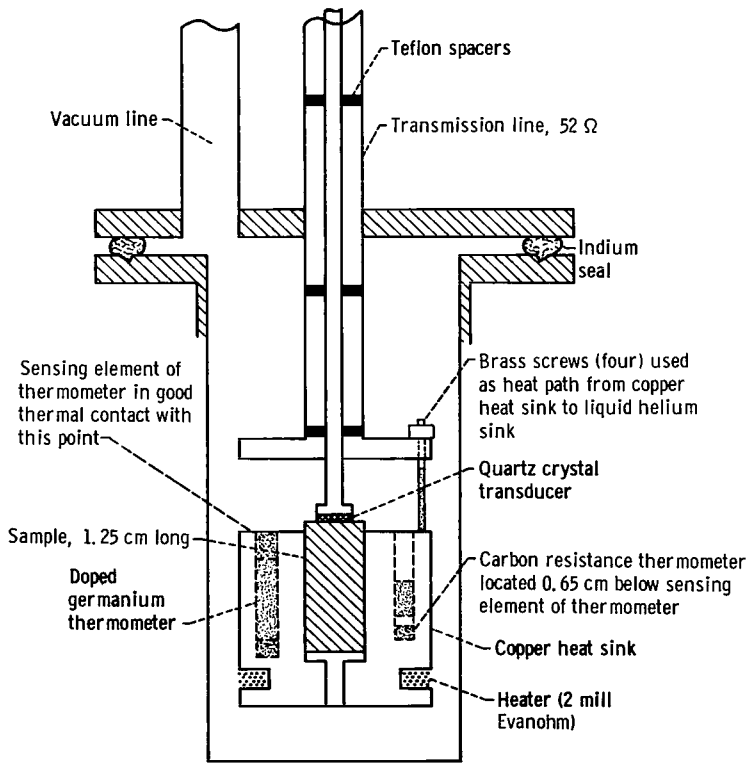

Figure 3. - Test chamber. Temperature can be varied from 1.6° to 77° K.

temperature test chamber, shown in figure 3, consists of an evacuated, stainless steel cylinder with a copper heat sink in the center. The niobium sample and the two resistors were located inside and were kept in good thermal contact with the copper cup. A heater of noninductively wound, Nylon-insulated, 0.002-inch-diameter heating-element wire was used to vary the temperature of the heat sink. By pumping on the liquid-helium vessel and varying the current through the heater, temperatures ranging from 1.6° to greater than 50° K are obtainable, although during the actual tests only temperatures as high as 9° K were needed. Heat paths to the helium bath were such that any desired temperature could be maintained for long periods of time by passing a constant direct current through the heater. The ultrasonic pulses were brought into the chamber through a 52-ohm transmission line composed of two concentric stainless steel tubes separated by polytetrafluoroethylene spacers. A copper piston pushed by a phosphor-bronze spring was then used to connect electrically the inner conductor of the line with the quartz crystal transducer. Quartz elements with fundamental frequencies of 30, 10, and 5 megahertz were used to generate the sound waves into the niobium crystals. Both longitudinal and transverse waves were studied. The stopcock grease used to couple the transducer to the sample worked well, particularly when a large pressure was applied to the seal prior to cool down. The background magnetic fields were supplied by a niobium-stannide superconducting coil which provided longitudinal fields.

The niobium samples tested varied in length from 1.14 to 1.05 centimeters and had a 0.92-centimeter diameter. Two 5-centimeter-long niobium rods were first oriented, one with its axis in the (100) crystal direction and the other with its axis in the (110) crystal direction, with an accuracy of better than $1/2^{\circ}$ as determined by X-ray backscattering measurements. Then a sparkcutter was used to cut the rods perpendicular to the desired crystal directions into 1.25-centimeter samples which were hand lapped. The rings used were stainless steel with faces flat and parallel to within 2.5 microns. However, parallelism of the faces became a problem in some cases despite careful hand lapping. The niobium specimens, which are body-centered-cubic, were oriented, some with their axes parallel to the (100) crystal direction and others with their axes parallel to the (110) crystal direction. Measured resistance ratios were used to indicate the purity of the various samples and their electronic mean free path. The samples had a resistance ratio ($R_{300^{\circ}\,K}/R_{4.2^{\circ}\,K}$) of 150, as measured by an energy-time-decay technique. One of the (110) samples was annealed for 10 hours at a temperature of 2200° C in a vacuum of 10^{-10} millimeter of mercury following a 4-hour oxygen treatment at 5×10^{-7} millimeter of mercury (ref. 20). The resulting resistance ratio was 1330. This sample had to be kept constantly at liquid-nitrogen temperature in order to avoid excessive oxidation of its surface and to reduce the mobility of impurities within it. Spectral analysis of the annealed and nonannealed samples revealed little difference in their impurity content. The analysis also indicated that the annealing process reduced

the amounts of hydrogen, potassium, iron, and several niobium compounds with carbon and oxygen, but it increased the percentage of oxygen and tungsten. In each case, the sample purity was higher than 99.9 percent.

MEASUREMENTS OF ULTRASONIC ATTENUATION

The temperature dependence of the attenuation was studied in niobium single crystals oriented in two directions, (100) and (110). Both longitudinal and transverse waves were used, and the frequency was varied from 30 to 330 megahertz. However, because of the impurity of the low-resistance-ratio material, the highest value obtainable, 330 megahertz, was still in the $q\ell \ll 1$ region, as indicated in figure 4 by the frequency square variation of the normal electronic attenuation (refs. 21 and 22). The annealed niobium sample showed a linear dependence of the attenuation on frequency above 170 megahertz (fig. 5) and thus was in the $q\ell > 1$ region (refs. 21 and 22).

Longitudinal Waves

Amplitude effects. - Amplitude dependence of the attenuation type observed by Love

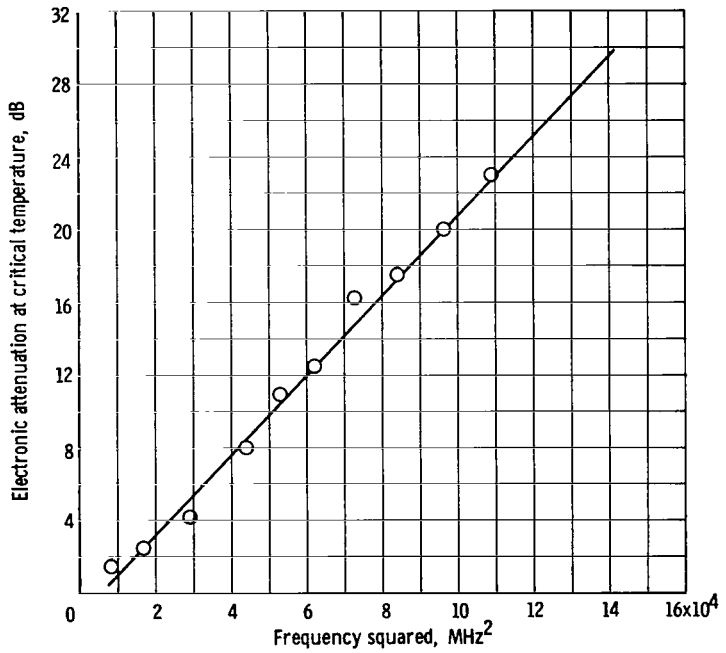

Figure 4. - Dependence of electronic attenuation on frequency for samples with resistance ratio of 150.

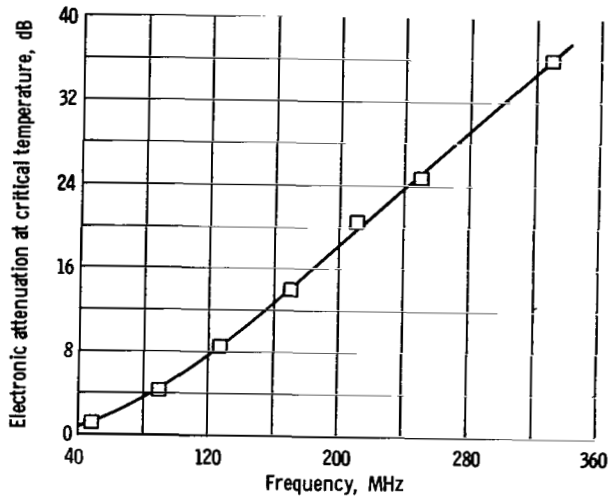

Figure 5. - Dependence of electronic attenuation on frequency for samples with resistance ratio of 1330.

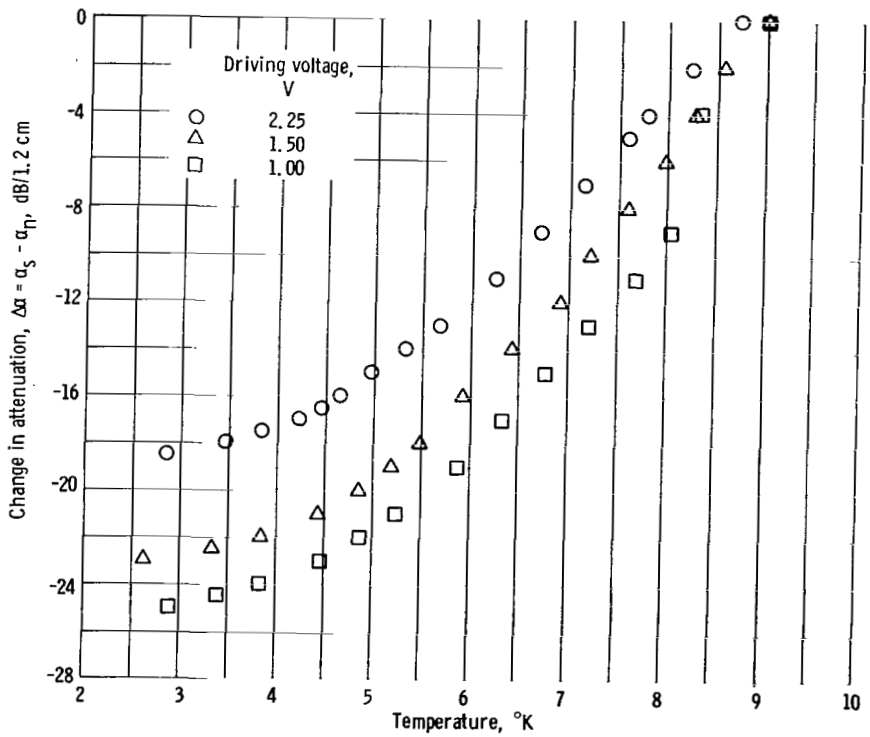

Figure 6. - Amplitude dependence of attenuation of longitudinal wave in annealed niobium (100) sample at 330 megahertz.

and Shaw (ref. 7) and by Tittmann and Bömmel (ref. 23) in lead was also found in the annealed niobium crystal. This crystal was studied in the (110) direction only. The energy input into the sample was varied by changing the amplitude of the initial wave transmitted to the transducer. Figure 6 shows plots of the measured values of the change in attenuation $\Delta\alpha = \alpha_s - \alpha_n$ against temperature for three different amplitudes and indicates a dependence of attenuation on energy input. The high-amplitude attenuation corresponds to a driving voltage of 2.25 volts, as measured at the oscillator, and corresponds to the highest output available. At this frequency, 330 megahertz, it is difficult to tell how much energy was actually transmitted to the crystal. Although the power limitation of the instrument restricted the range of measurement, it was obvious that an amplitude dependence effect was present in niobium, but the magnitude of the observed change was not as large as expected from the lead experiments. A small decrease in the critical temperature with increasing energy input was also observed. In all subsequent measurements presented in this report, as low an amplitude as was found feasible was used, and thus the error introduced was reduced. In the measurements of anisotropy, the amplitude of the initial pulse was carefully monitored so that it stayed the same in all cases. Tittmann and Bömmel (ref. 23) have presented an explanation of the amplitude effect which takes into account the influence of conduction electrons on dislocations in the lattice. According to their model, dislocations which are pinned down by impurities can be torn away with sufficiently large amplitude oscillations, and they will then vibrate around the nodes of the dislocation network. Since most electrons are in the superconducting state and are not scattered by the lattice, little electron damping occurs, and the dislocation lines are free to absorb energy from the sound wave. Thus, in order to obtain energy-gap measurements free of amplitude effect, waves of small amplitudes must be used. The presence of a magnetic field eliminates this amplitude effect, as shown by Love and Shaw (ref. 7). The amplitude effect could not be observed conclusively in any of the grain orientations of the unannealed crystals in the present study because of a lack of input energy range. However, it is expected that, since more dislocation lines are present in the unannealed samples, the amplitude dependence effect is present in them.

Energy gap. - Figure 7 shows for the three samples the variation of attenuation with reduced temperature for longitudinal ultrasonic waves having a frequency of 330 megahertz. Both the experimental data and the BCS theory show a sharp drop in the measured attenuation below the critical temperature, as shown previously for other metals. Good agreement was found among all three samples. The annealed sample shows somewhat closer agreement with the BCS curve than the others (fig. 7(c)). The energy gap for each specimen is then calculated from these curves by using equation (2)

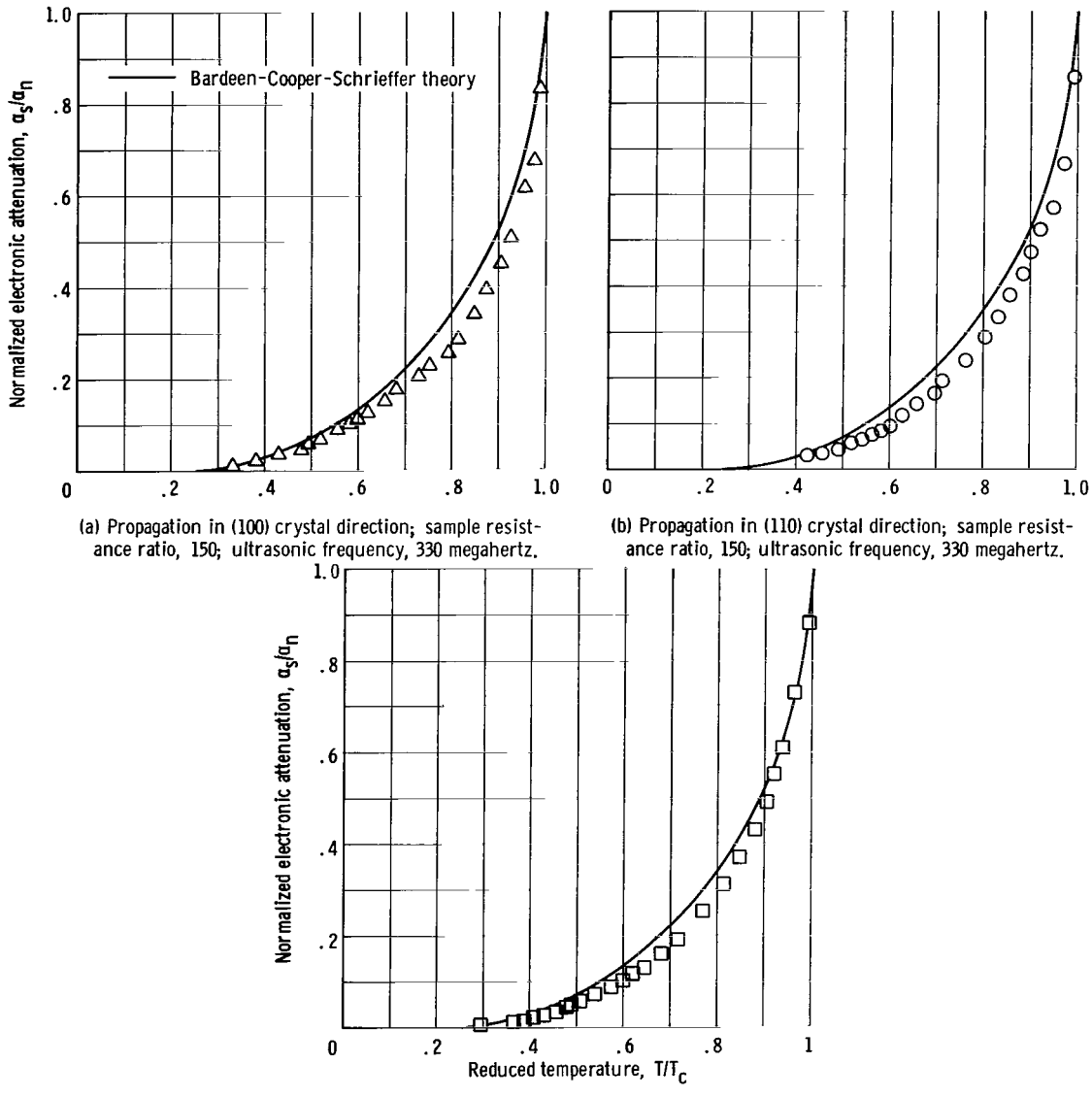

(a) Propagation in (100) crystal direction; sample resistance ratio, 150; ultrasonic frequency, 330 megahertz.

(b) Propagation in (110) crystal direction; sample resistance ratio, 150; ultrasonic frequency, 330 megahertz.

(c) Propagation in (110) crystal direction; sample resistance ratio, 1330; ultrasonic frequency, 330 megahertz.

Figure 7. - Variation of electronic attenuation in superconducting state as function of temperature for longitudinal waves.

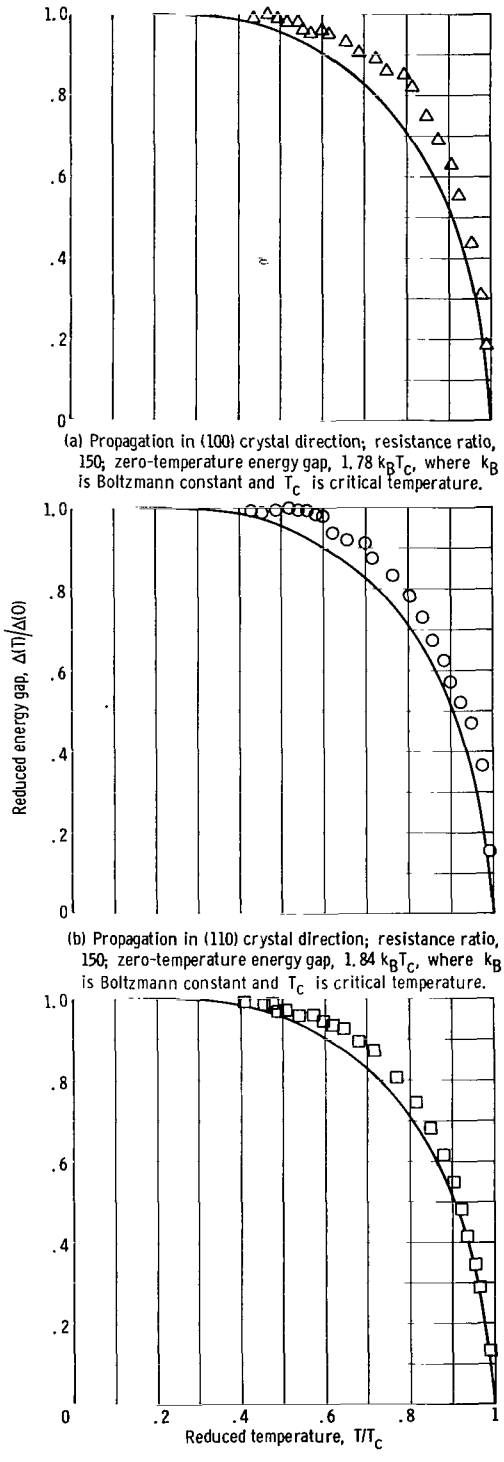

(a) Propagation in (100) crystal direction; resistance ratio, 150; zero-temperature energy gap, 1.78 $k_B T_c$, where k_B is Boltzmann constant and T_c is critical temperature.

(b) Propagation in (110) crystal direction; resistance ratio, 150; zero-temperature energy gap, 1.84 $k_B T_c$, where k_B is Boltzmann constant and T_c is critical temperature.

(c) Propagation in (110) crystal direction; resistance ratio, 1330; zero-temperature energy gap, 1.84 $k_B T_c$, where k_B is Boltzmann constant and T_c is critical temperature.

Figure 8. - Energy-gap dependence on temperature for longitudinal waves (eq. (2)).

$$\frac{\alpha_s}{\alpha_n} = \frac{2}{\exp\left[\frac{\Delta(T)}{k_B T}\right] + 1} \qquad (2)$$

and is plotted in figure 8. Again, better agreement is found between the theoretical gap variation and the annealed sample (fig. 8(c)), although all three crystals showed a dependence close to that predicted by the BCS theory. The zero-temperature energy-gap values were obtained by the method described by Morse, Olsen, and Gavenda (ref. 2). Plots of $\left[\ln(2\alpha_n/\alpha_s - 1)\right]^{-1}$ against reduced temperature T/T_c are shown in figure 9. The inverse of the slope of the extrapolated straight line for each curve at low reduced temperatures gives a direct measurement of the zero-temperature energy gap. Because of the high critical temperature of niobium, values of reduced temperature were easily reached beyond which the attenuation did not change measurably. These values eased the choice of a zero electronic attenuation level and were reflected in the linearity of the points of low temperatures and in the intercept of the extrapolated line at $T/T_c = 0$, which was the origin in every case (fig. 9), as predicted by equation (1). Accurate estimates of the zero-temperature energy gaps were obtained and these checked well with the extrapolated values obtained by extending the curve of $\Delta(T)$ against reduced temperature. The resulting values for $\Delta(0)$ showed a significant anisotropy in the gap between the (100) and (110) crystal directions:

$$2\Delta_{100}(0) = 3.56\ k_B T_c$$

$$2\Delta_{110}(0) = 3.68\ k_B T_c$$

The annealed (110) sample $q\ell > 1$ had the same value of $\Delta(0)k_B T_c$ as did the impure (110) sample $q\ell < 1$,

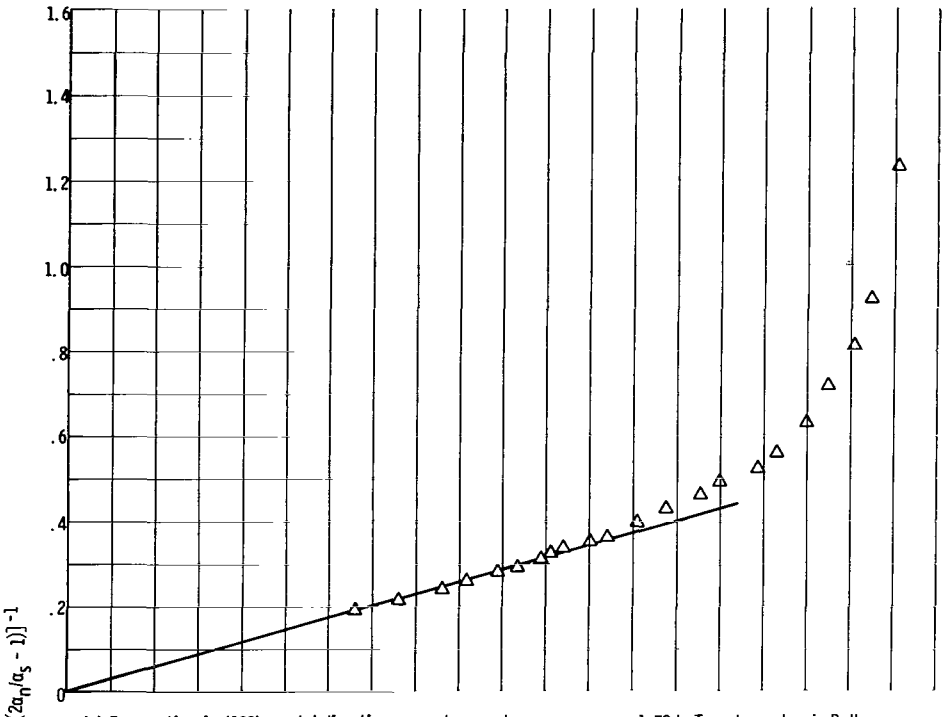

(a) Propagation in (100) crystal direction; zero-temperature energy gap, 1.78 $k_B T_c$, where k_B is Boltzmann constant and T_c is critical temperature; unannealed sample.

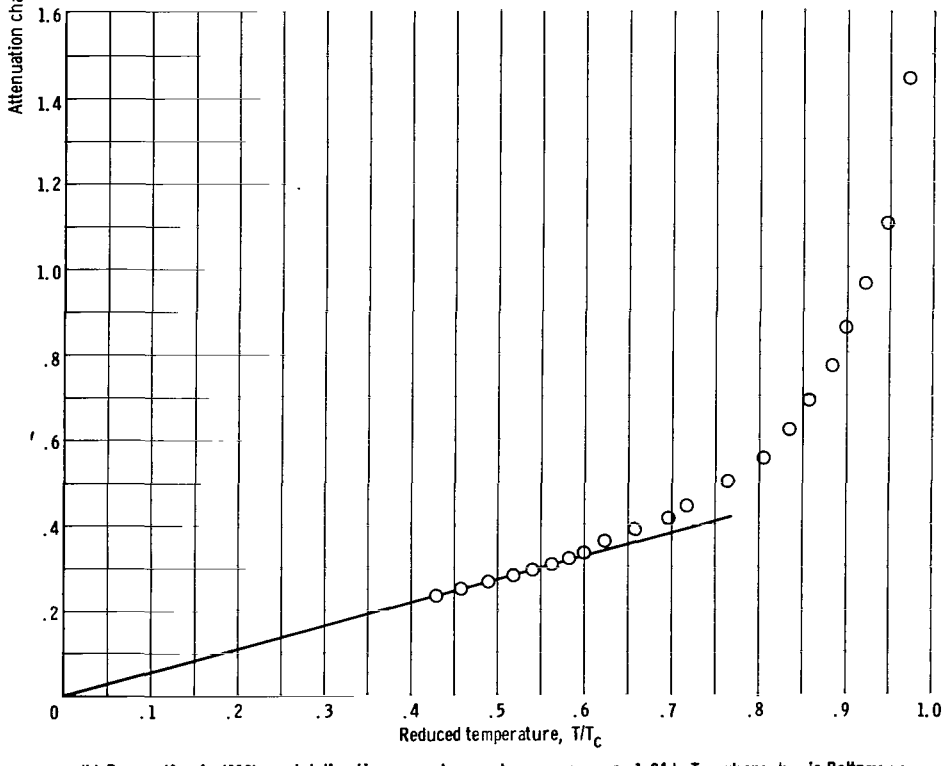

(b) Propagation in (110) crystal direction; zero-temperature energy gap, 1.84 $k_B T_c$, where k_B is Boltzmann constant and T_c is critical temperature; unannealed sample.

Figure 9. - Calculation of zero-temperature energy gap for longitudinal wave propagation.

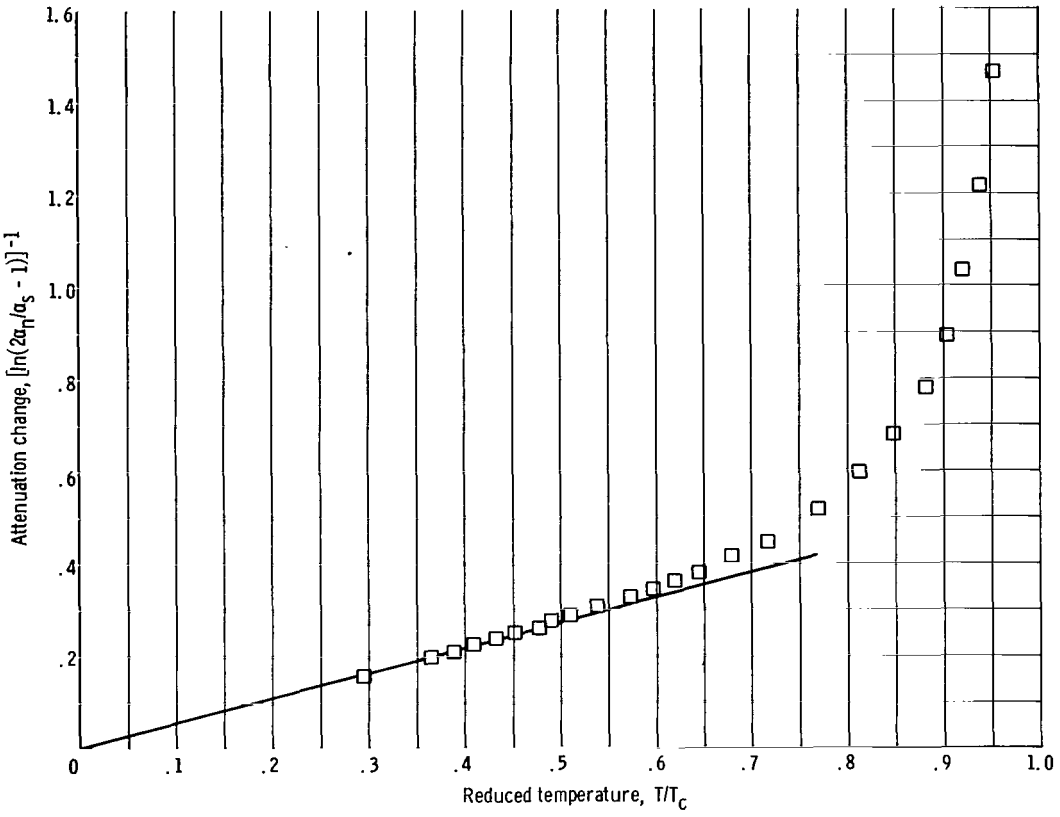

(c) Propagation in (110) crystal direction; zero-temperature energy gap, 1.84 $k_B T_c$, where k_B is Boltzmann constant and T_c is critical temperature; annealed sample.

Figure 9. - Concluded.

which supports Tsuneto's theory (ref. 15) that the BCS equation for attenuation of longitudinal waves is nearly independent of electronic mean free path. However, the critical temperature of the annealed sample was raised and its critical magnetic field lowered. The measured critical temperature of the unannealed crystals (resistance ratio of 150) was 8.67° K, whereas that of the annealed crystal (resistance ratio of 1330) was 9.04° K. Despite the low resistance-ratio values, these samples showed a behavior, in the case of longitudinal waves, close to that of an ideal superconductor, as described by theory (ref. 24).

The zero-temperature energy gap $2\Delta(0)$ of the (100) samples was $3.56\ k_B T_c$. This value agrees well with the BCS value of $3.52\ k_B T_c$ and $3.59\ k_B T_c$ (ref. 25), but is lower than other ultrasonic measurements ($3.77\ k_B T_c$ for the (100) direction, ref. 10) and thermal capacity data ($3.8\ k_B T_c$, ref. 26, and $3.9\ k_B T_c$, ref. 10). This value compares quite well with the tunneling value of 3.5 for a thin film system, niobium-niobium oxide-lead (ref. 27). It must be remembered, however, that thermal-capacity measurements give an averaged value of the energy gap over all crystal directions. The zero-

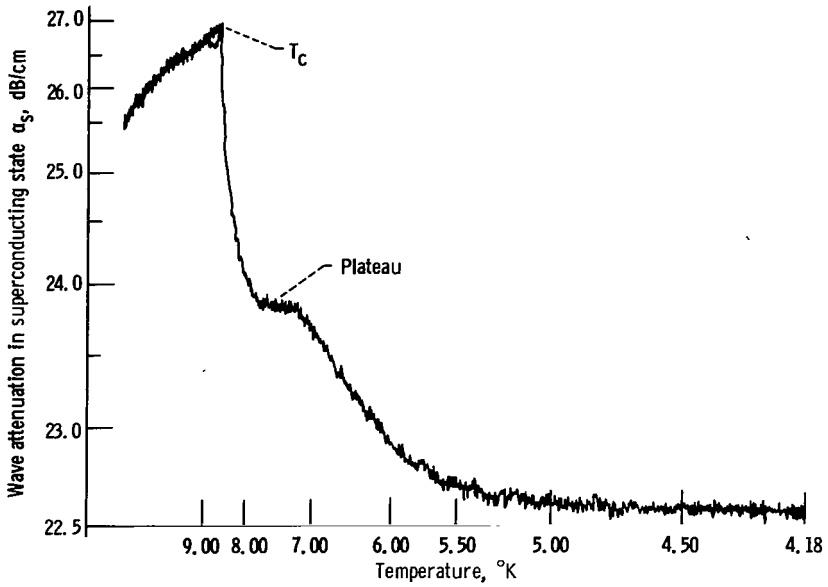

Figure 10. - Dependence of longitudinal wave attenuation in superconducting state. Sample oriented in (110) crystal direction; frequency, 50 megahertz.

temperature energy gap of the (110) sample was $3.68\ k_B T_c$, which agrees well with other longitudinal ultrasonic measurements of $3.68\ k_B T_c$ (ref. 10) but is lower than the shear-wave ultrasonic measurements of $3.8\ k_B T_c$ (ref. 11).

Attenuation plateau. - An anomalous effect similar to that observed by Claiborn and Einspruch (ref. 15) in niobium-zirconium alloys was seen in the (110) unannealed niobium crystal for longitudinal waves. A plateau occurred in the variation of the attenuation with temperature (fig. 10). This plateau spanned a large range of temperatures at low frequencies (50 to 30 MHz). Its width changed inversely with frequency and disappeared above 70 megahertz. The plateau was not observed in the annealed crystal and was, therefore, due to impurity and strains. Strains were the cause since the impurity content of the central portion of the sample was not highly reduced by the annealing process. Reference 13 pointed out that this behavior is indicative of the existence of low-frequency collective excitation modes in the energy gap around the Fermi surface in the plane perpendicular to the (110) crystal direction of the niobium crystal. This plateau, however, was not seen in the (110) crystal in the case of shear waves or in the (100) crystal with shear or longitudinal waves.

TRANSVERSE WAVES

The curves of figure 11 for shear waves at $q\ell$ values near unity (210 and 330 MHz) exhibit a distinctly different behavior from those of figure 7 for longitudinal waves.

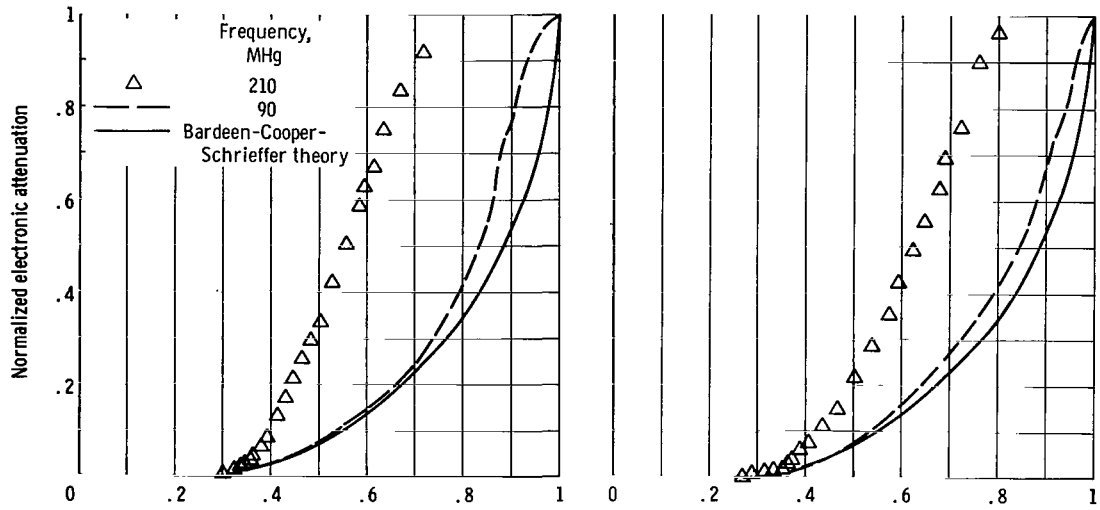

(a) Propagation in (100) crystal direction; sample resistance ratio, 150.

(b) Propagation in (110) crystal direction; sample resistance ratio, 150; polarization vectors in (100) crystal direction.

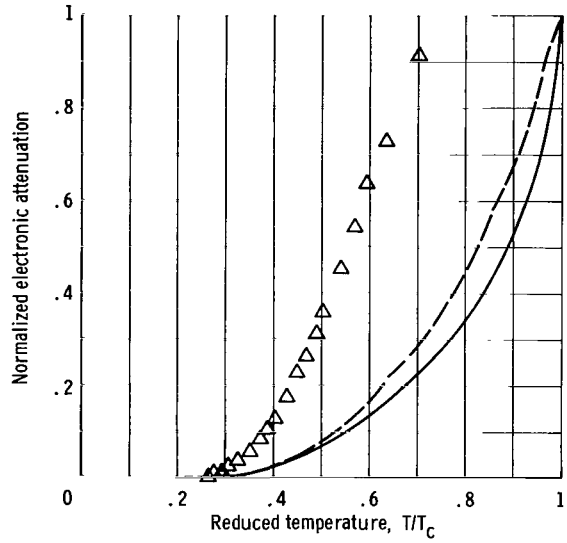

(c) Propagation in (110) crystal direction; sample resistance ratio, 1330; polarization vectors in (100) crystal direction.

Figure 11. - Variation of electronic attenuation in superconducting state as function of temperature for transverse alternating-current waves.

Instead of dropping abruptly, because of the Meissner effect, as the temperature was reduced below T_c, the attenuation ratio in figure 11 remained near its normal-state value until the temperature was lowered to the range 0.7 to 0.8 T_c; beyond 0.8 T_c a rapid drop ensued. This trend is somewhat similar to that predicted by Mackintosh (ref. 28) for shear waves at high frequencies. As in reference 28, the drop in attenuation below T_c sharpened and moved closer to T_c with decreasing ultrasonic frequency, as shown by the dashed lines in figure 11. In this case, the change in attenuation for a wave of 90 megahertz was close to the variation predicted by the BCS theory for longitudinal waves. As the temperature was decreased, the data of reference 11 showed a drop which occurred near T_c. Beyond the original drop, the remaining nonzero attenuation, called the "residual attenuation," is usually matched to the longitudinal BCS falloff (ref. 6). Reference 17 attributes such residual attenuation to a collision drag effect in which moving impurities collide with thermally excited, normal electrons. Whether such collisions could also cause the near normal attenuation in the region of the curves near T_c in figure 11 remains uncertain. Reference 11 used the residual-attenuation region at low reduced temperatures T/T_c to calculate a zero-temperature energy gap from the longitudinal BCS equation (2). However, attempts to make a similar analysis of the data of figure 11 at the high frequencies were unsuccessful because agreement with theory was obtained only at very low attenuations in the extremely low temperature region of $T/T_c < 0.30$. Although the apparatus was capable of reading T/T_c values of 0.18, the change in attenuation was too small to be recorded accurately. No thorough explanation of the behavior of shear waves in superconductors is yet available; thus, it is difficult to relate correctly the observed variation of attenuation with temperature to the energy-gap parameter.

Magnetic Field Effects

The effect of an external longitudinal magnetic field was similar for all samples and is shown for the (100) sample in figures 12, 13, and 14. Niobium, as was expected, behaved like a type I superconductor up to fields close to its critical field value. The Meissner effect was observed as the field was excluded from the sample, and the attenuation remained equal to its zero-field value at low temperatures. Upon reaching its critical temperature, the sample made a sharp transition to the normal state. In figures 6, 7, and 11, the plots of attenuation against temperature were obtained by slowly raising, rather than lowering, the temperature in order to avoid trapping flux when cooling down in a background magnetic field as shown in figure 14. The sharp increase in attenuation with increasing temperature at the critical point indicates that a first-order phase transition is taking place, in contrast to the field-free case, where a second-order phase transition

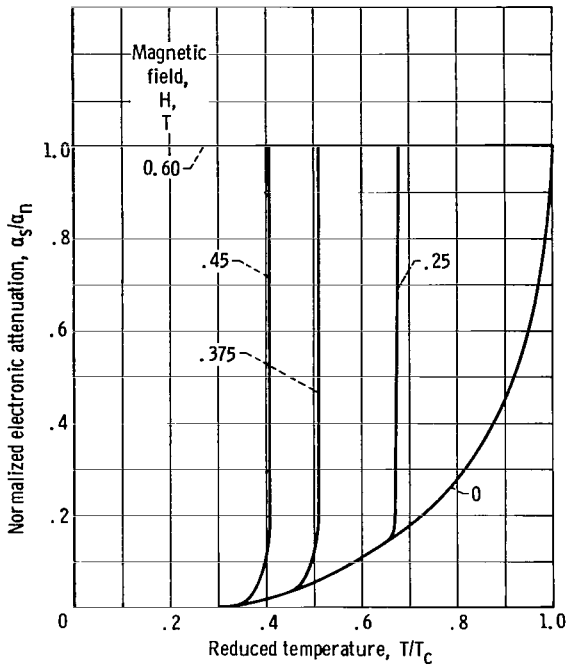

Figure 12. - Longitudinal-wave attenuation in (100) crystal direction for various background magnetic fields.

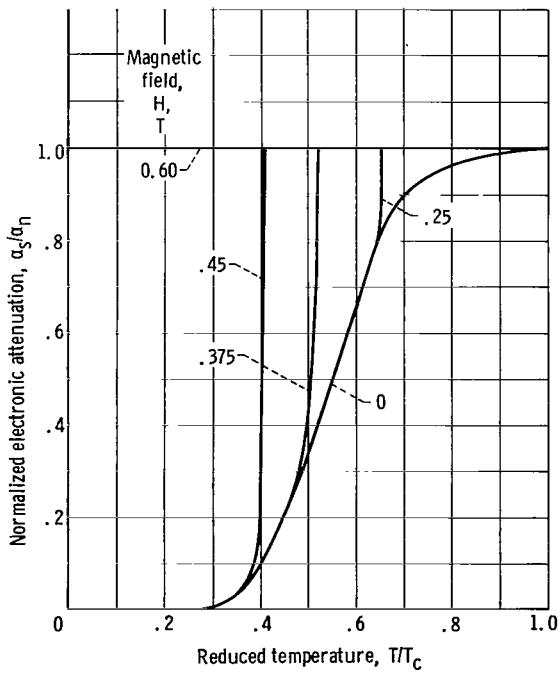

Figure 13. - Shear-wave attenuation in (100) crystal direction for various background magnetic fields.

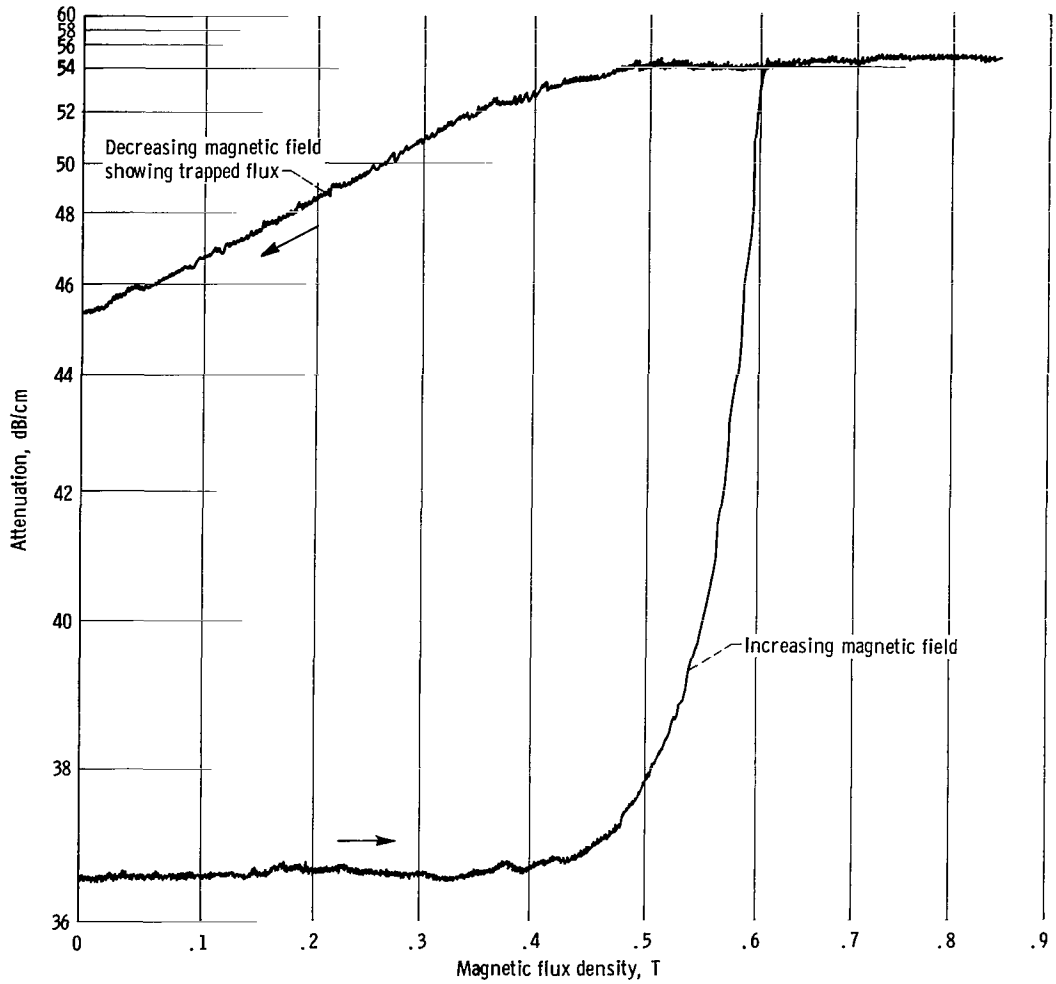

Figure 14. - Attenuation in (100) crystal direction in niobium sample as function of applied magnetic field. Frequency, 330 megahertz; temperature, 1.8° K.

is observed. Seen in high-background fields close to the critical magnetic field were flux jumps into the niobium, which consequently heated the sample. These flux jumps often caused the niobium to become normal by trapping increasing amounts of flux during each successive flux-jump-induced temperature cycle.

SUMMARY OF RESULTS

The attenuation of ultrasonic waves of frequencies of 30 to 330 megahertz was observed in niobium single crystals with a resistance ratio of 150 and an orientation in the (100) and (110) crystal directions. One of the (110) crystals was annealed, and its resistance ratio was raised to 1330 as measured by a coil decay technique. Both longitudinal and transverse waves were studied. In the case of longitudinal waves, the dependence of the electronic attenuation in the three crystals closely followed the Bordeen-Cooper-Schrieffer (BCS) theory except for small deviations near the critical temperature. Anisotrophy was shown in the zero-temperature energy gaps $\Delta(0)$ calculated from the attenuation data:

$$2\Delta_{100}(0) = 3.56\ k_B T_c$$

and

$$2\Delta_{110}(0) = 3.68\ k_B T_c$$

where k_B is the Boltzmann constant and T_c is the critical temperature. A dependence of extrapolated zero-temperature energy gap on input pulse amplitude was examined and found to exist in the niobium samples studied. However, the effect, was small, and meaningful measurements could be obtained for low amplitudes, as was seen in the reproducibility of all measurements and in the close agreement of experimental results with equation (1)(fig. 9). The values obtained for the zero-temperature energy gap compare well with values obtained through other measurements and with those predicted by the BCS theory. A study of the attenuation of low-frequency waves in the samples revealed the existence of collective excitation modes within the energy gap of the unannealed sample in the (110) direction. Both the annealed (110) sample ($q\ell > 1$, where q is wave number and ℓ is mean-free-path length) and the nonannealed (110) sample ($q\ell < 1$) had the same extrapolated zero-temperature energy gap and this supported Tsuneto's prediction that the BCS equation for attenuation of longitudinal waves is nearly independent of mean-free-path length.

The transverse shear waves had a near normal absorption for a range of temperatures

near the critical temperature. The absorption remained above the longitudinal BCS curve down to reduced temperatures of 0.30 for the case of high frequencies. A lack of existing models exhibiting this behavior of the attenuation prevented an estimation of the energy-gap parameters from the shear-wave attenuation observed.

The application of background magnetic fields reduced the transition temperature and caused first-order phase transitions to occur at the critical point for both longitudinal and shear waves. Flux trapping was also observed in the case of cool down of the sample below T_c in an applied field.

Lewis Research Center,
National Aeronautics and Space Administration,
Cleveland, Ohio, October 19, 1966,
129-02-05-02-22.

APPENDIX - SYMBOLS

$f(\epsilon)$ Fermi-Dirac function

$$= \frac{1}{\exp\left(\frac{\epsilon}{k_B T}\right) + 1}$$

H magnetic field

H_c critical magnetic yield

k_B Boltzmann constant

l mean free path length

q wave number

T absolute temperature

T_c critical temperature

T/T_c reduced temperature

α_n attenuation of wave in normal state

α_s attenuation of wave in super conducting state

Δ energy-gap parameter

REFERENCES

1. Bardeen, J.; Cooper, L. N.; and Schrieffer, J. R.: Theory of Superconductivity. Phys. Rev., vol. 108, no. 5, Dec. 1, 1957, pp. 1175-1204.

2. Morse, R. W.; Olsen, T.; and Gavenda, J. D.: Evidence for Anisotropy of the Superconducting Energy Gap from Ultrasonic Attenuation. Phys. Rev. Letters, vol. 3, no. 1, July 1, 1959, pp. 15-16.

3. Bezuglyĭ, P. A.; Galkin, A. A.; and Korolyuk, A. P.: Investigation of the Anisotropy of the Energy Gap in Superconducting Tin. Soviet Phys. JETP, vol. 12, no. 1, Jan. 1961, pp. 4-7.

4. Shepelev, A. G.; and Filimonov, G. D.: An Investigation of Energy Gap Anisotropy in Superconducting Tin. Soviet Phys. JETP, vol. 21, no. 4, Oct. 1965, pp. 704-708.

5. David, R.; and Poulis, N. J.: Ultrasonic Attenuation in Superconducting Aluminum. Proceedings of the 8th International Conference on Low Temperature Physics. R. O. Davies, ed., Butterworth, Inc., London, 1963, pp. 193-194.

6. Morse, R. W.: Ultrasonic Attenuation in Superconductors. I. B. M. J., vol. 6, no. 1, Jan. 1962, pp. 58-62.

7. Love, R. E.; and Shaw, R. W.: Ultrasonic Attenuation in Superconducting Lead. Rev. Mod. Phys., vol. 36, no. 1, Jan. 1964, pp. 260-263.

8. Love, R. E.; Shaw, R. W.; and Fate, W. A.: Attenuation of Longitudinal Ultrasound in Superconducting Lead. Phys. Rev., vol. 138, no. 5A, May, 1965, pp. 1453-1460.

9. Dobbs, E. Roland; and Perz, John M.: Anisotropy of the Energy Gap in Niobium from Ultrasonic Measurements. Rev. Mod. Phys., vol. 36, no. 1, Jan. 1964, pp. 257-260.

10. Dobbs, E. R.; and Perz, J. M.: Ultrasonic Determination of the Energy gap in Superconducting Niobium. Proceedings of the 8th International Conference on Low Temperature Physics. R. O. Davies, ed., Butterworth, Inc., London, 1963, pp. 195-196.

11. Levy, Moises; Kagiwada, Reynold; and Radnick, Isadore: Ultrasonic Measurements in Three Superconducting Transition Metals. Proceedings of the 8th International Conference on Low Temperature Physics. R. O. Davies, ed., Butterworth, Inc., London, 1963, pp. 188-190. Also: Ultrasonic Attenuation of Transverse Waves in V, Nb, and Ta for $q\ell < 1$. Phys. Rev., vol. 132, no. 5, Dec. 1963, pp. 2039-2046.

12. Bohm, H. V.; and Horwitz, N. H.: Ultrasonic Attenuation in Superconducting Vanadium and Zinc. Proceedings of the 8th International Conference on Low Temperature Physics. R. O. Davies, ed., Butterworth, Inc., London, 1963, pp. 191-192.

13. Claiborne, Lewis T.; and Einspruch, Norman G.: Ultrasonic Absorption by Superconducting Nb-Zr Alloys. Phys. Rev., vol. 132, no. 2, Oct. 1963, pp. 621-629.

14. Morse, R. W.: Ultrasonic Attenuation in Metals at Low Temperatures. Progress in Cryogenics. Vol. 1. K. Mendelssohn, ed., Heywood and Co., Ltd., London, 1959, pp. 219-259.

15. Tsuneto, T.: Ultrasonic Attenuation in Superconductors. Phys. Rev., vol. 121, no. 2, Jan. 1961, pp. 402-415.

16. Bohm, H. V.; and Morse, R. W.: Ultrasonic Attenuation in Superconductors: Dependence on Electron Mean Free Path. Am. Phys. Soc. Bull., Ser. II, vol. 3, no. 3, May 1958, p. 225.

17. Tsuneto, Toshihiko: Shear Wave Attenuation in Superconductors. Rutgers University, Nov. 1964. (Available from DDC as AD-609052.)

18. Chick, Bruce; Anderson, George; and Truell, Rohn: Ultrasonic Attenuation Unit and Its Use in Measuring Attenuation in Alkali Halides. J. Acoust. Soc. Am., vol. 32, no. 2, Feb. 1960, pp. 186-193.

19. Clement, J. R.; and Quinnell, E. H.: The Low Temperature Characteristics of Carbon-Composition Thermometers. Rev. Sci. Inst., vol. 23, no. 5, May 1952, pp. 213-216.

20. Taylor, G.; and Christian, J. W.: The Effect of High Vacuum Purification on the Mechanical Properties of Niobium Single Crystals. Acta Met., vol. 13, no. 11, Nov. 1965, pp. 1216-1218.

21. Pippard, A. B.: Ultrasonic Attenuation in Metals. Phil. Mag., vol. 46, no. 381, Oct. 1955, pp. 1104-1114.

22. Pippard, A. B.: Theory of Ultrasonic Attenuation in Metals and Magneto-acoustic Oscillations. Roy. Soc. Proc., vol. 257, no. 1289, Sept. 6, 1960, pp. 165-193.

23. Tittmann, B. R.; and Bömmel, H. E.: Amplitude-Dependent Ultrasonic Attenuation in Superconducting Lead. Phys. Rev. Letters, vol. 14, no. 9, Mar. 1, 1965, pp. 296-298.

24. Bardeen, J.; and Schrieffer, J. R.: Recent Developments in Superconductivity. Progress in Low Temperature Physics. Vol. III. C. J. Gorter, ed., Interscience Publ., Inc., 1961, pp. 170-287.

25. Sherrill, M. D.; and Edwards, H. H.: Superconducting Tunneling on Bulk Niobium. Phys. Rev. Letters, vol. 6, no. 9, May 1, 1961, pp. 460-461.

26. Mendelssohn, K.: Experimental Work on Superconductivity. I. B. M. J., vol. 6, no. 1, Jan. 1962, pp. 27-30.

27. Townsend, P.; and Sutton, J.: A Study of Superconducting Niobium by Electron Tunnelling. Phys. Soc. Proc., vol. 78, pt. 2, Aug. 1961, pp. 309-311.

28. Mackintosh, A. R.: Shear Wave Attenuation in Normal and Superconducting Tin. Proceedings of the 7th International Conference on Low Temperature Physics. G. M. Graham and A. C. Hollis Hallett, eds., University of Toronto Press, 1961, pp. 240-243.

"The aeronautical and space activities of the United States shall be conducted so as to contribute . . . to the expansion of human knowledge of phenomena in the atmosphere and space. The Administration shall provide for the widest practicable and appropriate dissemination of information concerning its activities and the results thereof."

—NATIONAL AERONAUTICS AND SPACE ACT OF 1958

NASA SCIENTIFIC AND TECHNICAL PUBLICATIONS

TECHNICAL REPORTS: Scientific and technical information considered important, complete, and a lasting contribution to existing knowledge.

TECHNICAL NOTES: Information less broad in scope but nevertheless of importance as a contribution to existing knowledge.

TECHNICAL MEMORANDUMS: Information receiving limited distribution because of preliminary data, security classification, or other reasons.

CONTRACTOR REPORTS: Technical information generated in connection with a NASA contract or grant and released under NASA auspices.

TECHNICAL TRANSLATIONS: Information published in a foreign language considered to merit NASA distribution in English.

TECHNICAL REPRINTS: Information derived from NASA activities and initially published in the form of journal articles.

SPECIAL PUBLICATIONS: Information derived from or of value to NASA activities but not necessarily reporting the results of individual NASA-programmed scientific efforts. Publications include conference proceedings, monographs, data compilations, handbooks, sourcebooks, and special bibliographies.

Details on the availability of these publications may be obtained from:

SCIENTIFIC AND TECHNICAL INFORMATION DIVISION

NATIONAL AERONAUTICS AND SPACE ADMINISTRATION

Washington, D.C. 20546